

**DEVELOPMENT AND VALIDATION
OF A US SIDE IMPACT
MOVEABLE DEFORMABLE BARRIER FE MODEL**

Abdullatif K. Zaouk and Dhafer Marzougui

*FHWA/NHTSA National Crash Analysis Center
The George Washington University
20101 Academic Way
Ashburn, VA 20147
USA*

Phone: (703) 726-8348

Fax: (703) 726-8359

E-mail: zaouk@ncac.gwu.edu

ABSTRACT

Automotive safety regulations vary in different parts of the world. Dynamic side impact regulations, for example, are different than the ones in Europe. United States National Highway Traffic Safety Administration (NHTSA) and the European Union (EU) have each produced their own distinct testing procedures such as different deformable barriers, impact configurations and anthropomorphic test devices (dummies). Although both test procedures have the same final objective, estimate occupant responses in side impact, they differ greatly in execution. One of the main differences in testing is the Moving Deformable Barrier (MDB) used. The US MDB is designed to represent an average midsize vehicle in the US market, while the European MDB represents a mid size vehicle in Europe.

The objective of this paper is to develop a finite element model representing the US deformable barrier for use in side impact simulations. Special emphasis is made on using the various available material models in LS-DYNA and the correct adhesive properties to predict the correct behavior of the honeycomb material. These models are validated to available full-scale tests.

As known by many researchers, the main difficulty of MDB modeling is the prediction of the barrier complex failure modes. In side impact tests, the severe shear deformation of the honeycomb material, full densification of barrier edge, rupture of aluminum cover sheets, and tearing of honeycomb blocks are often observed. This complex pattern of honeycomb material failure mode makes it difficult to predict. Numerical instabilities, such as negative volume, sever hourglassing, and inaccurate predictions are often experienced.

INTRODUCTION

Automotive accidents account for approximately 41,471 fatalities and 3.2 million injuries per year (average 1988-1997). The average annual incidence of tow-away light vehicle crashes in all light vehicles is approximately 3 million with about 4.6 million occupants involved. Approximately 600,000 are involved in side crashes exposing 920,000 occupants to such crashes, and accounting for about 11,300 fatalities (30 percent) yearly (NASS/CDS 1988-1997) [2].

The US dynamic side impact requirement, FMVSS-214, is used to evaluate the performance of passenger vehicles in car-to-car side crashes [1]. The standard was phased in beginning in 1994 and applies to all 1997 cars. It mimics a car-to-car side impact where the struck car is stationary and the striking car, represented by a deformable barrier, is moving. The test configuration as specified by the National Highway Traffic Safety Administration (NHTSA) is shown in figure 1. Schematically, a moving deformable barrier (MDB) is shown impacting the side of a stationary vehicle at 54 km/h (33.5 mph). The MDB is towed at a crabbed angle of 27° to its longitudinal axis. This configuration is intended to simulate a striking generic vehicle moving at 48.4 km/h (30 mph), perpendicular to the side of the struck vehicle traveling at 24.2 km/h (15 mph). The crabbed angle configuration allows the simulation of a two-vehicle side impact, both in motion condition, using a simplified test method where only one vehicle is in motion.

NHTSA's Side Impact Dummies (SIDs) are placed in the front and rear seating positions on the struck side of the stationary test vehicle. They represent a 50th percentile male, and are belted. FMVSS-214 injury criteria is as follows [1]:

- TTI ≤ 85 g's (for 4 door vehicle) or TTI ≤ 90 g's (for 2 door vehicle)
- Pelvic Acceleration ≤ 130 g's (for all vehicles)

Where the Thoracic Trauma Index (TTI) is defined as follows:

$$\bullet \text{TTI} = (G_R + G_{LS})/2,$$

Where G_R is the greater peak lateral acceleration of the upper or lower ribs expressed in g's and the G_{LS} is the lower spine peak acceleration also expressed in g's.

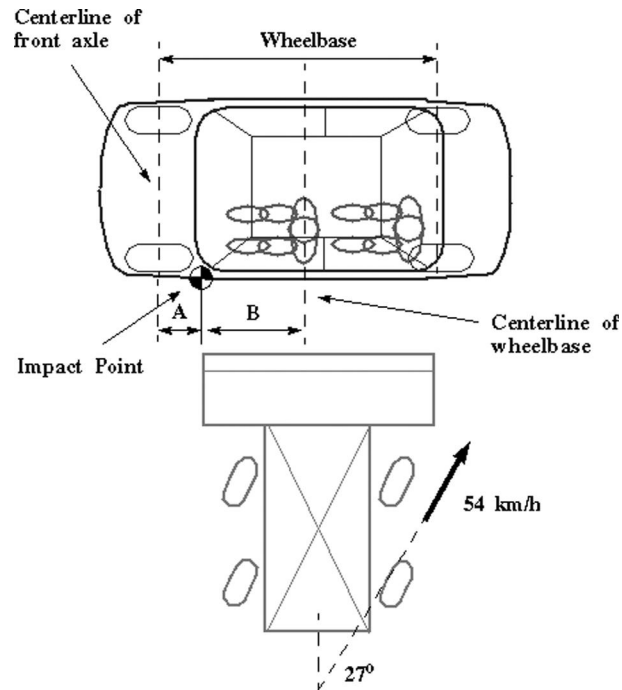


Figure 1. FMVSS-214 test procedure

The NHTSA MDB represents an average passenger vehicle in the US. Figure 2 shows the MDB's specifications. The MDB consists of the following components [1]:

- Main frame assembly
- Barrier face
- Hub assembly
- Rear guide assembly
- Axle assembly
- Camera mounts and ballast

The MDB, including the impact surface, supporting structure, and carriage weighs 1,368 kg (3,015 lbs), has a track width of 1,880 mm (74 in.) and a wheelbase of 2,591 mm (102 in.). It has the following center of gravity [1]:

X = 1,123 mm (44.2 in.) rear of front axle

Y = 7.7 mm (0.3 in) left of longitudinal center

Z = 500 mm (19.7 in.) from the ground

With the following moments of inertia:

Pitch = 2,263 kg-m² (1,669 ft-lb-sec²)

Roll = 508 kg-m² (375 ft-lb-sec²)

Yaw = 2572 kg-m² (1,897 ft-lb-sec²)

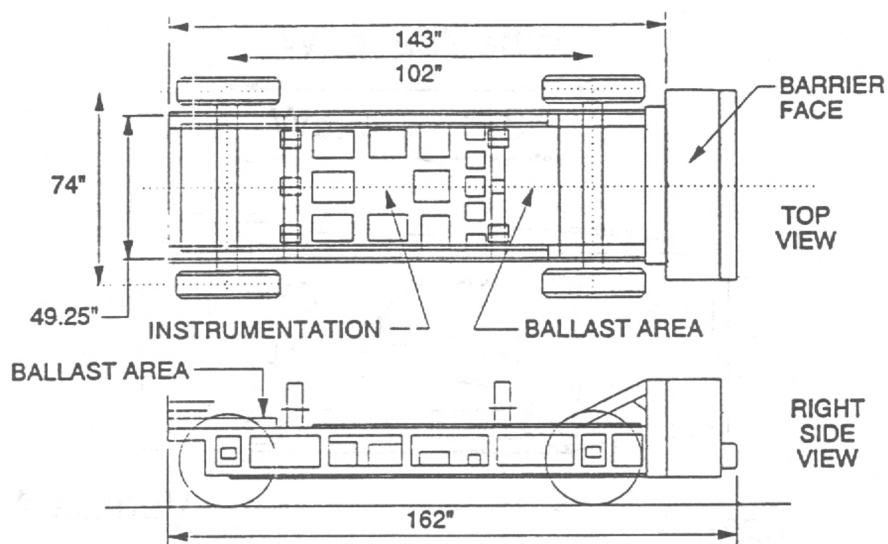


Figure 2. Moveable Deformable Barrier (MDB) specifications [1]

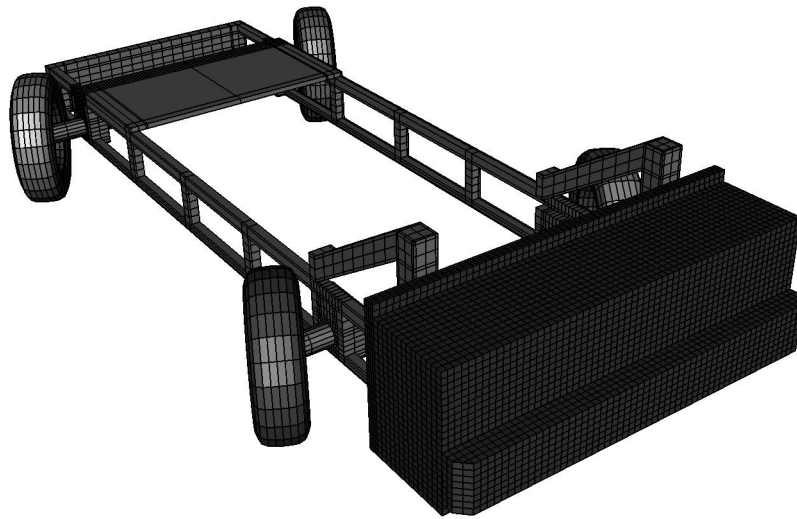


Figure 5. NCAC FE model of the NHTSA moveable deformable barrier

Table 1. FE model information

| Component Name | Material Models |
|-----------------------|----------------------------|
| Bumper | MAT_HONEYCOMB (26) |
| Main-Block | MAT_HONEYCOMB (26) |
| Mounting-Plate | MAT_RIGID (20) |
| MDB-Chassis | MAT_RIGID (20) |
| Bumper-Shell | MAT_NULL (9) |
| Main-Block-Shell | MAT_NULL (9) |
| Bumper-Front-Plate | MAT_PLATSTIC_KINEMATIC (3) |
| Bumper-Back-Plate | MAT_PLATSTIC_KINEMATIC (3) |
| Main-Block-Face | MAT_PLATSTIC_KINEMATIC (3) |
| Main-Block-Face- | MAT_PLATSTIC_KINEMATIC (3) |
| Mounting-Block-S | MAT_NULL (9) |
| Tires | MAT_VISCOELASTIC (6) |
| Rims | MAT_PLATSTIC_KINEMATIC (3) |
| Hubs | MAT_ELASTIC (1) |

The new barrier face is composed of 8 components (figure 6). Both honeycomb blocks are covered by shell elements sharing the same nodes (merged), with null material properties. The null materials are used instead of solid elements when defining a contact interface. Table 2 shows the material properties used for both the main block and bumper [3]. The bumper uses a stiffer honeycomb property compared to the main block.

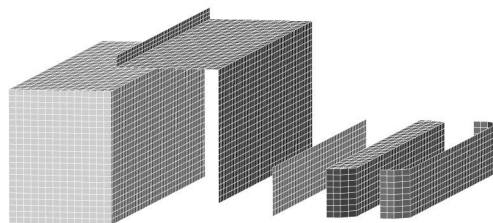


Figure 6. Exploded view of the NCAC FE barrier face

Table 2. Honeycomb material properties

| MAT_HONEYCOMB | Honeycomb_245psi | Honeycomb_45psi |
|------------------------------------|-----------------------------|-----------------------------|
| Density | 8.50 E-11 t/mm ³ | 2.62 E-11 t/mm ³ |
| Young's Modulus | 68950 MPa | 68950 MPa |
| Poisson's Ratio | 0.33 | 0.33 |
| Yield Stress | 160 MPa | 160 MPa |
| Relative Volume (compacted) | 0.031 | 0.009 |
| Elastic Modulus Eaau | 1020 MPa | 172 MPa |
| Elastic Modulus Ebbu | 340 MPa | 57.2 MPa |
| Elastic Modulus Eccu | 340 MPa | 57.2 MPa |
| Shear Modulus Gabu | 434 MPa | 145 MPa |
| Shear Modulus Gbcu | 214 MPa | 75 MPa |
| Shear Modulus Gcau | 434 MPa | 145 MPa |

Two different aluminum material properties are used in the MDB, 2024-T3 and 5052-H34 (figure 3). Table 3 shows the material properties used for the Aluminum face.

Table 3. Aluminum face material properties

| MAT_PLASTIC_KINEMATIC | 2024-T3 | 5052-H34 |
|--|----------------------------|-----------------------------|
| Density | 2.78E-09 t/mm ³ | 2.68 E-09 t/mm ³ |
| Young's Modulus | 72400 MPa | 70000 MPa |
| Poisson's Ratio | 0.33 | 0.33 |
| Yield Stress | 345 MPa | 215 MPa |
| Plastic Tang. Hardening Modulus | 777 MPa | 450 MPa |
| Hardening Parameter | 0.5 | 0.5 |

As previously mentioned, all components of the actual MDB are bonded together with the exception of the main block face which is bonded to the main block at the lower vertical location, and connected to the mounting block at the upper vertical location using bolts (figure 7). To simulate these bonded connections, the CONTACT_TIEBREAK_NODES TO SURFACE option in LS-DYNA is used. This option allows for modeling normal and shear failure, and thus simulating an adhesive between two components. At this time, the failure parameters are not defined due to the lack of adhesives data. The bond between the different components is assumed not to fail. However, in the near future testing will be conducted to extract these parameters and implement them into the FE model.

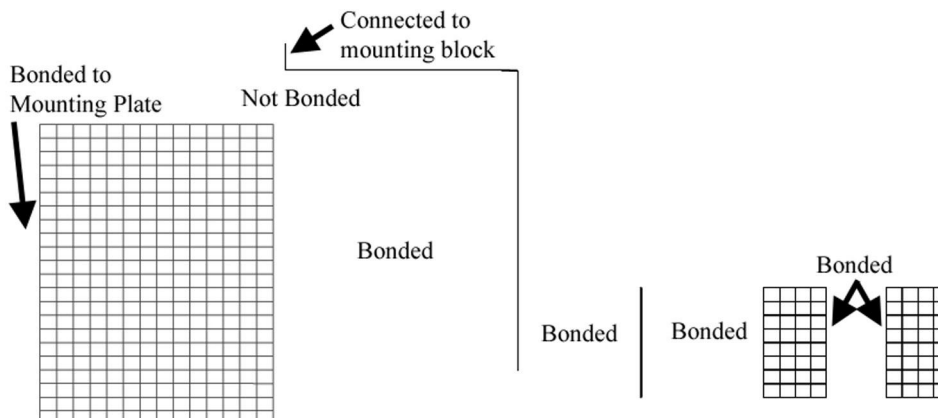


Figure 7. Barrier face connections

Table 4 shows the center of gravity location (C.G), the moments of inertia and weight for both the FE model and the FMVSS-214 requirement listed previously. The FE model is reasonable in comparison with the FMVSS-214 requirement. This confirms the accuracy of the geometry and weight distribution.

Table 4. C.G. and Moments of Inertia comparison

| | FMVSS-214 | FE Model |
|--------------------------|-----------|----------|
| C.G Location | | |
| CGx (mm) | 1,123 | 1,068 |
| CGy (mm) | 8 | 2 |
| CGz (mm) | 500 | 486 |
| Total weight (kg) | 1,368 | 1,388 |

FE MODEL VALIDATON

As part of the validation process, simulations with the new MDB FE model are compared to available full-scale tests. Test number V1068 conducted by NHTSA at the Vehicle Research and Test Center is used in this study. In this test, the MDB was towed into a fixed load cell barrier at a perpendicular angle. The impact speed of the test was 40.2 km/h (25 mph), with the MDB crabbed at a 26° angle. The fixed load cell barrier was composed of 36 loads cells in a 4 rows x 9 columns configuration (figure 8). The barrier was at 66 mm (2.6 in.) from the ground.

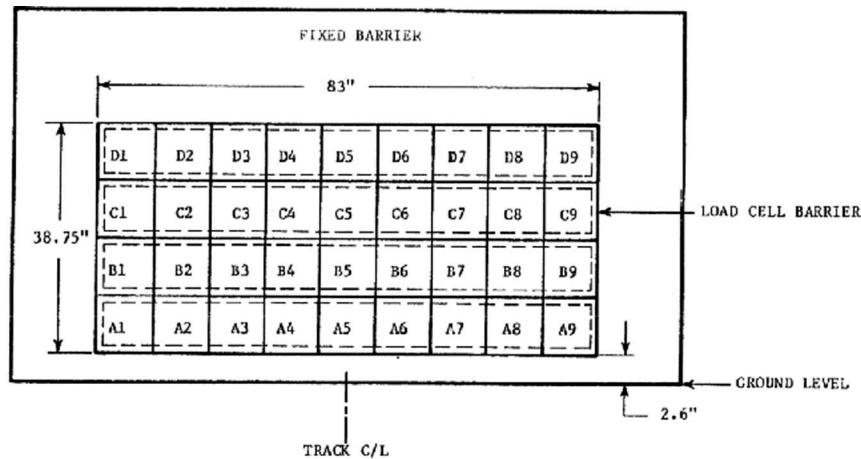


Figure 8. Load cell barrier configuration

Using the RIGIDWALL_PLANAR_FINITE option in LS-DYNA, a load cell barrier composed of 36 rigid walls was created to replicate the load cell barrier in test V1068. The simulation was performed on a Silicon Graphics Origin 2000 system shared memory, SMP super computer consisting of 16 processors. The SMP version of the LS-DYNA, version 950 was used. The simulation was run for 150 milliseconds of impact using 6 processors. The CPU time for the run was 10 hours. The simulation was performed using a fixed time step of 1 microsecond was used. The acceleration records and rigid wall forces were computed every 0.05 milliseconds. An SAE-60 filter was used to reduce numerical noise effects in the simulation.

The general deformation of the barrier in the simulation can be compared visually to the images captured from the full-scale crash test with the high-speed cameras. Figures 9 and 10 show side and top views of the MDB at the initial state, 36 msec., and 150 msec. It can be observed from the figures that finite element model accurately represents the barrier deformation seen in the full-scale crash test

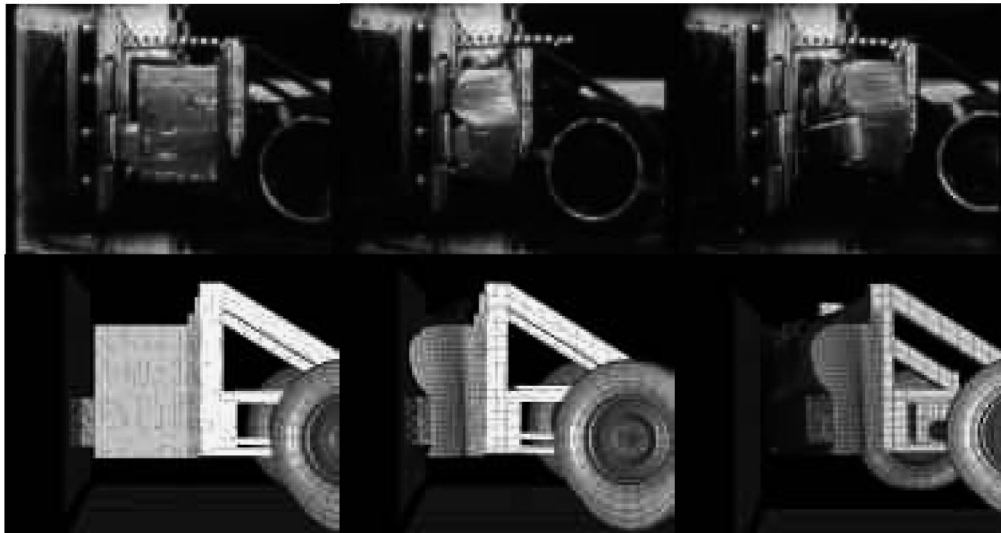


Figure 9. Side view of the MDB deformation for FE model and test

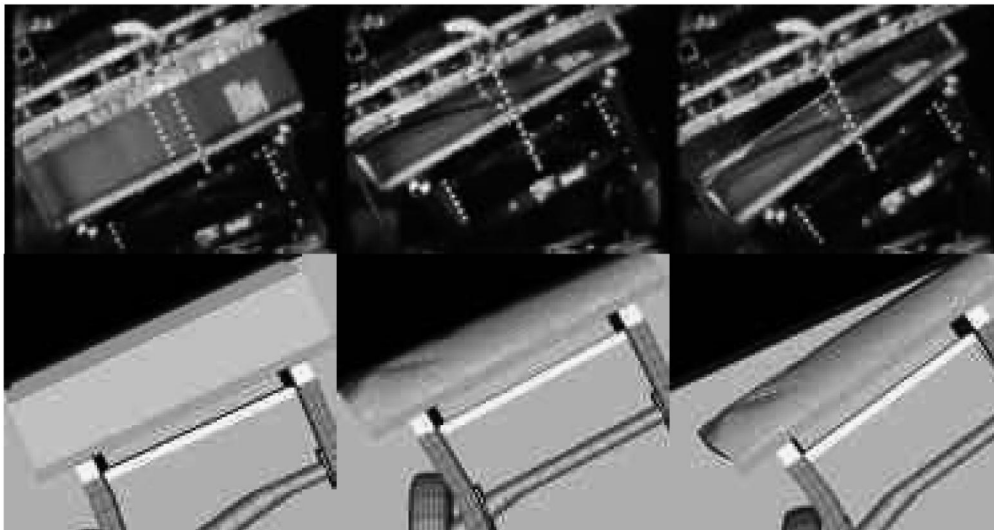


Figure 10. Top view of the MDB deformation for FE model and test

The next level of comparison is the velocity and acceleration time histories at the MDB center of gravity location. Figures 11 and 12 show the comparison of the acceleration and velocity records respectively between test and simulation. It can be observed from the curves that the simulation results are in excellent agreement with the full-scale crash test data

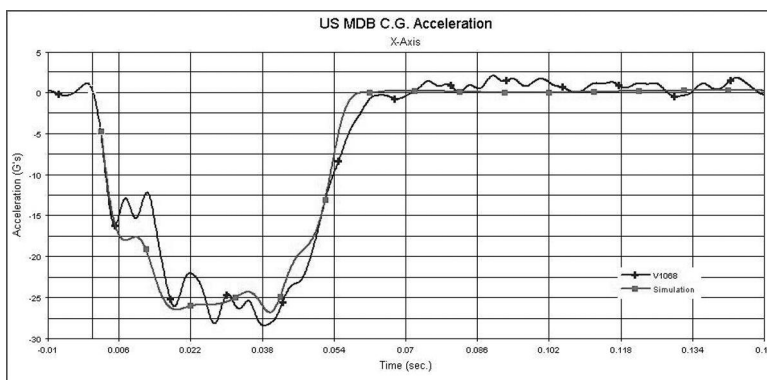


Figure 11. MDB center of gravity acceleration

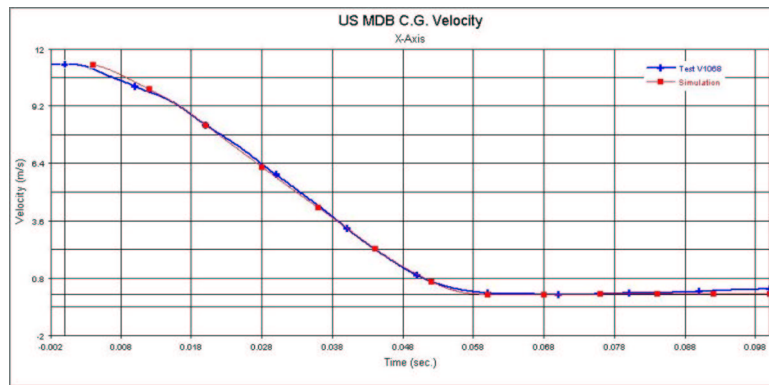


Figure 12. MDB center of gravity velocity

The final level of comparison is the load cell force. As previously mentioned, the fixed load cell barrier is composed of 36 load cells in a 4 rows x 9 columns configuration (figure 8). In the data analysis, the forces from the load cells are grouped as follows:

- Group 1 – A1 thru A9
- Group 2 – B1 thru B9
- Group 3 – C1 thru C9
- Group 4 – D1 thru D9

Figure 13 shows the simulation and full-scale crash test forces collected for group 2. Here, the forces are the sum of the total forces measured by the 9-load cell array in the second row, and represents those forces normal to the impacted fixed barrier. The comparison shows a reasonable agreement between the test and simulation. However, the FE model is less compliant. This could be attributed to the material properties used in the model. The maximum force seen by the load cell barrier is 272 KN for the FE model compared to 231 KN for the test (table 5).

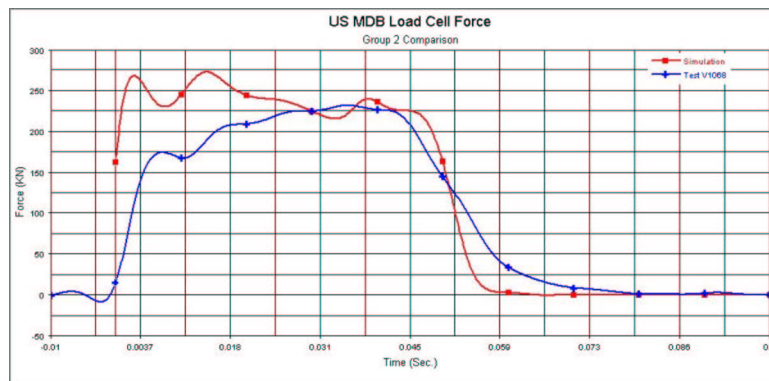


Figure 13. Group-2 load cell force comparison

Table 5. Load cell barrier summary

| Position | Test | | Simulation | |
|----------------|-------------|----------|-------------|----------|
| | Time (msec) | Max (KN) | Time (msec) | Max (KN) |
| Group 1 | 6.38 | 29.06 | 4.00 | 24.59 |
| Group 2 | 35.50 | 231.55 | 13.80 | 272.48 |
| Group 3 | 42.50 | 122.39 | 35.80 | 146.33 |
| Group 4 | 10.88 | 11.18 | 46.40 | 7.33 |
| Total | 34.75 | 380.03 | 37.20 | 384.84 |

Figure 14 shows the load cell force comparison of group 3 between test and simulation. Similarly, the forces are the sum of the total forces measured by the 9-load cell array in the third row, and represents those forces normal to the impacted fixed barrier. The curve shapes and peak values show reasonable correlation and consistency. The maximum force seen by the load cell barrier is 122 KN for the FE model compared to 146 KN for the test (table 5).

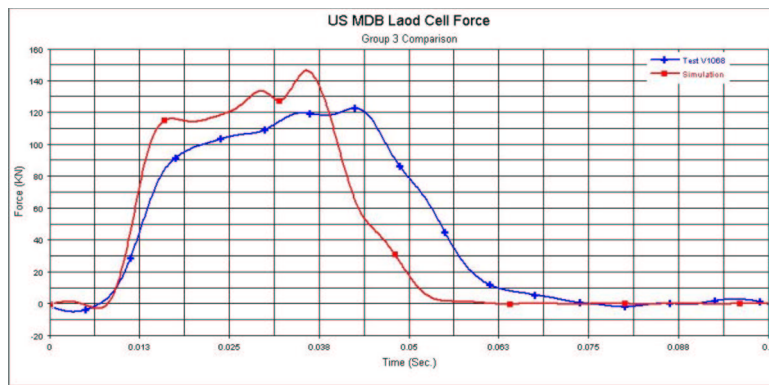


Figure 14. Group-3 load cell force comparison

Figure 15 shows the total load cell force comparison between test and simulation. The forces are the sum of the total forces measured by the 36-load cell array, and represents those forces normal to the impacted fixed barrier. It can be observed that the curve shapes and peak values show good correlation and consistency. The maximum force seen by the load cell barrier is 384 kN for the FE model compared to 380 kN for the test (table 5).

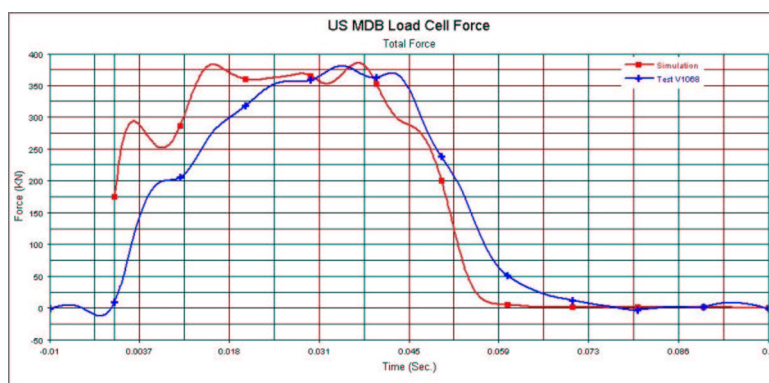


Figure 13. Total load cell force comparison

CONCLUSION

A finite element model of the US MDB was developed and the simulation results were compared to the full-scale crash test. The simulation showed consistent results compared with the full-scale test. The simulated overall profile of the barrier section matches that of the test very well. The magnitude of the acceleration curves from the simulation compared very favorably with those obtained from the test. Similarly, the general trend of the load cell forces compared reasonably well with those obtained from the test. Observations of the crash test film and rendered simulation playback (not included in the paper) indicate that the model captured the motion and characteristics of the surrogate vehicle.

The simulation results presented in this paper are preliminary and show a first attempt at such prediction. Further improvement in the model, and validations against other tests, will enhance its fidelity and its ability to accurately predict the behavior under various impact conditions.

ACKNOWLEDGEMENT

The authors wish to thank Mr. Steve Summers from the National Highway Safety Administration for his valuable help in providing test data. Funding for this research project was provided by Ford Motor Company.

REFERENCES

1. Federal Register, Part II 49 CFR Part 571, section 214 et. al. "Federal Motor Vehicle Safety Standards; Side Impact Protection", October 1, 1997
2. Zaouk, A. K., Eigen, A. M. and Digges, K., "Occupant Injury Patterns in Side Crashes; SAE International Congress and Exposition, Paper # 2001-01-0723.
3. "Mechanical Properties of Hexcel Honeycomb Materials" Hexcel Corporation, TSB 120